# A Comparative Study of PI, RST and ADRC Control Strategies of a Doubly Fed Induction Generator Based Wind Energy Conversion System

Mohssine Chakib*‡, Ahmed Essadki*, Tamou Nasser**

*Electrical Engineering Department of High School of Technical Education (ENSET), Mohammed V University, BP 6207 Rabat, Morocco

**Communication Networks Department, High National School of Computer Science and Systems Analysis (ENSIAS), Mohammed V University, BP 713, Rabat, Morocco

(chakib1mohssine@gmail.com, ahmed.essadki1@gmail.com, tamounasser@gmail.com)

‡ Corresponding Author; Mohssine Chakib, Rabat, Morocco, Tel: +212 679 316 075,

chakib1mohssine@gmail.com

*Received: 06.03.2018 Accepted: 08.04.2018*

**Abstract-** This paper presents a comparative study between three controllers for a Doubly Fed Induction Generator (DFIG) integrated into a wind turbine system. This work also aims to present a new control strategy called the Active Disturbance Rejection Control (ADRC) based on the extended state observer (ESO). In order to evaluate its performances, the proposed ADRC controller is compared with the PI and the robust RST controllers. Therefore, the active and reactive powers between the stator of DFIG and the grid are controlled independently by using the three control strategies, the first is the ADRC, the second is the classical Proportional-Integral (PI) and the third called polynomial RST controller. First, a modeling of wind turbine and DFIG is presented. Also, in order to maximize the power of wind energy conversion, the use of MPPT control is indispensable. Then, these three control strategies are designed, simulated and their performances were tested and compared in terms of instruction tracking and robustness. The simulations were realized by MATLAB/Simulink software.

**Keywords** Active Disturbance Rejection Control (ADRC); DFIG; Extended State Observer (ESO); PI controller; RST controller; MPPT.

## 1. Introduction

In recent years, there has been an evolution of the electricity production based on wind energy. As a result, the wind energy is the subject of several researches [1]. Although this energy source is inexhaustible, environmental friendly and it has developed thanks to the diversity of exploitable zones its relatively interesting cost as well as its sensibility to grid parameters and its efficiency is still low compared to conventional sources [2-3].

The doubly fed induction generator (DFIG) is broadly used for variable speed wind power generation system thanks to its several advantages over other generators. These advantages are easiness of speed control, operation at over a large range of wind speeds of 30% around the synchronous speed and an inverter rated at 25-30% of the total system power [3-5]. Contrary, the DFIG is subject to many constraints, such as the effects of parametric uncertainties (due to overheating, saturation ...) and the disturbance of the speed variation, which could divert the system from its optimal functioning. Therefore, the control of DFIG has become a very important research subject and several control strategies were established [6-7].

In order to remedy the disadvantages of the classical PI controller that suffers many limitations [6-8], the RST controller has three individual polynomials chosen so as to reduce the effect of disturbance in reference signal tracking. The synthesis of this regulator is an algorithm sophisticated based on pole placement technique [9-10]. In addition, a new control strategy called the active disturbance rejection

control (ADRC) founded by Han in 1995 is adopted in order to ensure the decoupling of the system from the actual disturbance acting on the plant [11].

The purpose of this work is to evaluate and compare the performance of the ADRC control strategy based on the extended state observer (ESO) with the classical PI and the robust RST controllers. These three controllers were used to control of rotor side converter RSC in order to control the active and reactive powers exchanged between the stator of DFIG and the grid controller. The results of simulation under MATLAB/Simulink environment prove the robustness of this new regulator against parameters variations of the generator; they also show its performance in terms of the reference tracking.

This paper will include three main parts: The first part will be devoted to modeling of the components of the Wind Energy Conversion System (DFIG, wind turbine, ....) and the principle of MPPT control (Maximum Power Point Tracking). In the second part, we will introduce the theoretical analysis and modeling of the three control strategies (PI, RST and ADRC). Then these controllers were developed to control the stator active and reactive power of DFIG in order to maximize the wind energy production. Finally, in the third part, the simulation results will be presented by using MATLAB/Simulink software, discussed and compared. Finally, we terminate by a conclusion.

## 2. Description and Modeling of the Wind Energy Conversion System

Our wind energy conversion system, which is shown in "Fig.1", consists of: a wind turbine, gearbox, DFIG, two converters and the rotor side controller (RSC) [3-6].

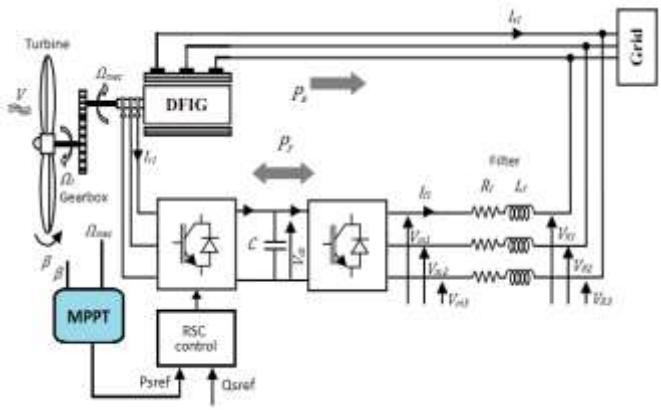


**Fig. 1.** Model of the variable speed wind turbine conversion chain.

### *2.1. Wind Turbine*

The turbine transforms the wind energy into a mechanical energy and the aerodynamic power available on a wind turbine rotor [11-14], this power is given by:

$$P_{aer} = \frac{1}{2} C_p(\lambda, \beta) \rho \pi R^2 V^3 \quad (1)$$

Where ρ is the air density, R is the turbine radios and V is the wind velocity.

The power coefficient $C_p$ is given by the following equation [4, 16]:

$$C_p(\lambda, \beta) = C_1\left(\frac{C_2}{\lambda_i} - C_3\beta - C_4\right)e^{\left(-\frac{C_5}{\lambda_i}\right)} + C_6\lambda \quad (2)$$

Where:

$$\lambda = \frac{\Omega_t R}{V} \quad ; \quad \frac{1}{\lambda_i} = \frac{1}{\lambda + 0.08\beta} - \frac{0.035}{1+\beta^3} \quad (3)$$

$C_1$=0.5176, $C_2$=116, $C_3$=0.4, $C_4$=5, $C_5$=21, $C_6$=0.0068

$\lambda$ is the speed ratio and $\Omega_t$ is the mechanical speed of the turbine.

The mechanical model between the turbine and shaft generator is defined by [4, 9-10, 19]:

$$T_{mec} = J\frac{d\Omega_g}{dt} = T_g - T_{em} - f_v\Omega_g \quad (4)$$

Where $J = \frac{J_t}{G^2} + J_g$

Where $T_g$, $T_{em}$ and $T_{mec}$ are respectively the torque of the fast shaft, the electromagnetic torque and the mechanical torque of generator, J is the total moment of inertia depends on the inertia of the generator $J_g$ and the inertia of the turbine $J_t$ and $f_v$ is the viscous friction coefficient, and $\Omega_g$ is the mechanical speed of the generator.

The next figure represents the block diagram model of the wind turbine:

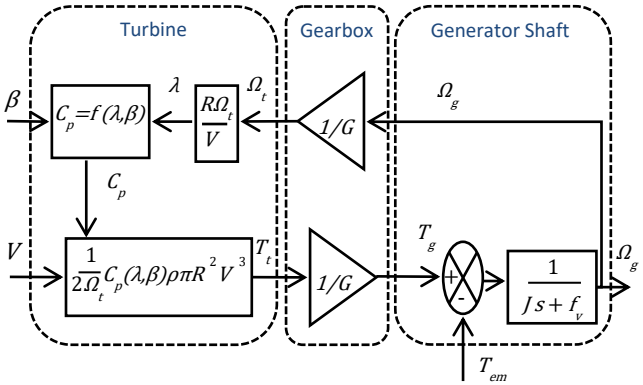


**Fig. 2.** Block diagram model of the turbine

### *2.2. Wind Turbine with MPPT*

To extract the maximum power generated, we must fix the speed ratio to its optimal value $\lambda_{opt}$ and the power coefficient to its maximum value $C_{pmax}$ [4, 8, 13].

The value of wind speed is estimated by the following equation [11].

$$\hat{v} = \frac{R\hat{\Omega}_t}{\lambda_{opt}} \quad (5)$$

The electromagnetic torque reference is determined by the following equation [11]:

$$T_{em-ref} = \frac{1}{2G\Omega_t} C_{pmax} \rho \pi R^2 \hat{v}^3 \quad (6)$$

The next figure represents the model of the turbine with MPPT:

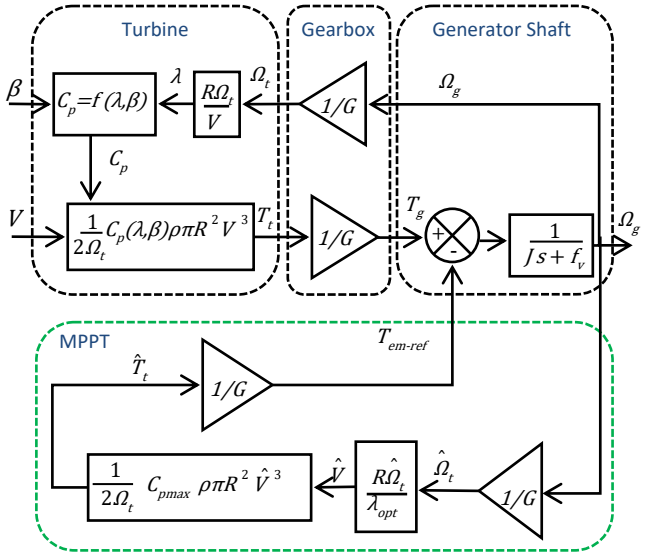


**Fig. 3.** Block diagram model of the turbine with MPPT

*2.3. Wind Turbine*

The back to back converter allows bidirectional transit of power between the rotor side (RSC) and grid side (GSC). These converters are controlled by the PWM control which the mathematical model of these converters represented by the following system of equations [10].

$$\begin{bmatrix} V_{ra} \\ V_{rb} \\ V_{rc} \end{bmatrix} = \frac{U_{dc}}{3} \begin{bmatrix} 2 & -1 & -1 \\ -1 & 2 & -1 \\ -1 & -1 & 2 \end{bmatrix} \begin{bmatrix} S_a \\ S_b \\ S_c \end{bmatrix} \quad (7)$$

Where, $V_{rabc}$ and $S_{abc}$ are respectively the output voltages and the control signals of the inverter.

Figure 4 shows the model of back to back converter.

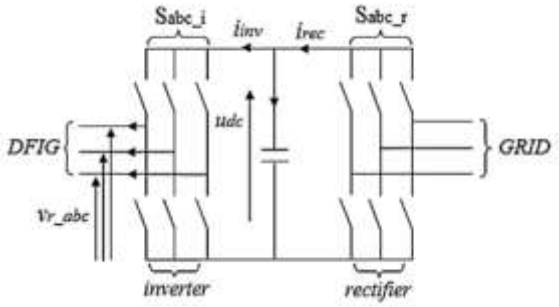


**Fig. 4.** Model of back to back converter

*2.1. Modeling of the DFIG*

The modeling of DFIG is described in the Park reference frame. The following equation system describes the overall modeling of the generator [3-4, 6, 24].

The electrical voltages are given by the following equations:

$$\begin{cases} V_{ds} = R_s I_{sd} + \frac{d\phi_{sd}}{dt} - \omega_s \phi_{sq} \\ V_{qs} = R_s I_{sq} + \frac{d\phi_{sq}}{dt} + \omega_s \phi_{sd} \\ V_{dr} = R_r I_{rd} + \frac{d\phi_{rd}}{dt} - \omega_r \phi_{rq} \\ V_{qr} = R_r I_{rq} + \frac{d\phi_{rq}}{dt} + \omega_r \phi_{rd} \end{cases} \quad (8)$$

The stator and rotor flux are given in the "equation 9":

$$\begin{cases} \phi_{ds} = L_s I_{sd} + M I_{rd} \\ \phi_{qs} = L_s I_{sq} + M I_{rq} \\ \phi_{dr} = L_r I_{rd} + M I_{sd} \\ \phi_{qr} = L_r I_{rq} + M I_{sq} \end{cases} \quad (9)$$

The electromagnetic torque is also expressed as a function of currents and flux "Eq.10":

$$T_{em} = p\frac{M}{L_s}(\phi_{sd} I_{rq} - \phi_{sq} I_{rq}) \quad (10)$$

The expression of the active and reactive power in the stator is:

$$\begin{cases} P_s = V_{sd} I_{sd} + V_{sq} I_{sq} \\ Q_s = V_{sq} I_{sd} - V_{sd} I_{sq} \end{cases} \quad (11)$$

*2.4. Modeling of vector control of the DFIG*

In order to control the production of electricity of a variable speed wind system, we will perform an independent control of the active and reactive power by establishing the equations that link the rotor voltages generated by an inverter to the active and reactive powers of the stator [8, 10].

For simplification reasons, we have adopted a stator flux aligned on the d-axis [8, 10, 15]. Therefore:

$$\begin{cases} \phi_{ds} = \phi_s = L_s I_{ds} + M I_{dr} \\ \phi_{qs} = 0 = L_s I_{qs} + M I_{qr} \end{cases} \quad (12)$$

Assuming that the electrical grid is stable, this leads to a constant stator flux $\phi_s$. In addition, stator resistance $R_s$ can be neglected since this is a realistic assumption for the high power generators used in the wind turbine [8, 18, 21]. On the basis of these assumptions, we obtain "Eq.13":

$$\begin{cases} V_{ds} = 0 \\ V_{qs} = V_s = \omega_s . \phi_s \end{cases} \quad (13)$$

The adaptation of these equations to the simplifying assumptions gives a new expression of the active and reactive power "Eq.14":

$$\begin{cases} P_s = -V_s \frac{M}{L_s} I_{qr} \\ Q_s = -V_s \frac{M}{L_s} I_{dr} + \frac{V_s^2}{L_s \omega_s} \end{cases} \quad (14)$$

For power control of DFIG, the expressions of the rotor voltages are established according to the rotor currents "Eq.15".

$$\begin{cases} V_{dr} = R_r I_{dr} + L_r \sigma \frac{dI_{rd}}{dt} - g\omega_s L_r \sigma I_{qr} \\ V_{qr} = R_r I_{qr} + L_r \sigma \frac{dI_{rq}}{dt} - g\omega_s L_r \sigma I_{rd} + g\omega_s \frac{V_s M}{L_s \omega_s} \end{cases} \quad (15)$$

Where: $\sigma = 1 - \frac{M^2}{L_s L_r}$

According to these assumptions, the electromagnetic torque of the DFIG is given as follows:

$$T_{em} = p\frac{M}{L_s}\phi_{sq} I_{rq} \quad (16)$$

These equations have been grouped to form a simplified model of DFIG.

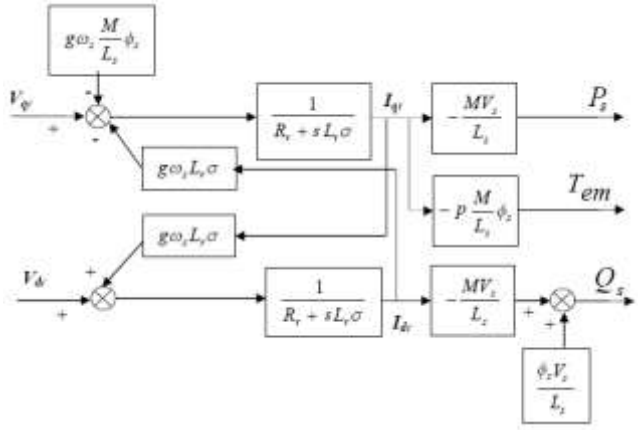

**Fig. 5.** Simplified Theoretical Model of DFIG.

## 3. Design and Synthesis of Controllers and Their Application to the DFIG

### *3.1. Proportional Integral (PI) Controller*

Proportional-Integral controller is a combination of both actions proportional and integral in order to cancel the static error. The structure of a parallel PI controller system is represented in "Fig.6" [7-8, 17-18].

The derivative action of PID controller is excluded because it is characterized by amplifying the effect of system noise.

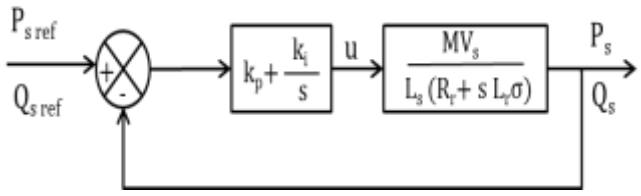

**Fig. 6.** Structure of PI controller system for the DFIG.

The open loop transfer function is:

$$G(s) = \left(k_p + \frac{k_i}{s}\right)\left(\frac{MV_s}{L_s(R_r + s L_r\sigma)}\right) = \frac{s+\frac{k_i}{k_p}}{\frac{s}{k_p}} \frac{\frac{MV_s}{L_s L_r\sigma}}{s+\frac{R_r}{L_r\sigma}} \quad (17)$$

We use the method of poles compensation for the synthesis of the regulator in order to eliminate the zero present on the transfer function [7-8, 10, 20]. We pose:

$$\frac{k_i}{k_p} = \frac{R_r}{L_r\sigma} \quad (18)$$

Thus:

$$G(s) = \frac{k_p \frac{MV_s}{L_s L_r\sigma}}{s} = \frac{1}{\tau_r s} \quad (19)$$

Where $\tau_r$ is response time:

$$\tau_r = \frac{1}{k_p}\frac{L_s L_r\sigma}{MV_s} \quad (20)$$

In closed loop we will have:

$$F(s) = \frac{1}{1+\tau_r s} \quad (21)$$

Therefore, the parameters $k_p$ and $k_i$ of PI controller are given by:

$$\begin{cases} k_p = \frac{1}{\tau_r}\frac{L_s L_r\sigma}{MV_s} \\ k_i = \frac{1}{\tau_r}\frac{R_r L_s}{MV_s} \end{cases} \quad (22)$$

We chose: $\tau_r = 10$ ms

Fig. 7 shows the PI control structure applied to the rotor side converter in order to control the stator active and reactive powers of the DFIG.

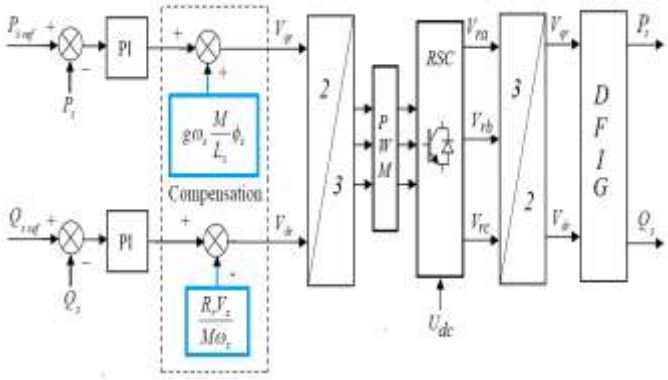

**Fig. 7.** Scheme of power control of DFIG using PI controller.

### *3.2. Polynomial RST Controller*

RST comes from the name of three polynomials R(s), S(s) and T(s) must be determined in order to obtain an efficient control. The structure of the RST controller system is represented in "Fig.8" [10, 22-23].

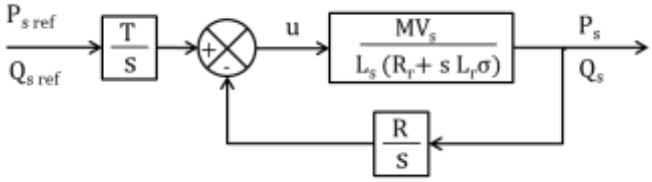

**Fig. 8.** Structure of RST controller system for the DFIG.

The principle of pole placement is to specify an arbitrary polynomial D(s) and to calculate the polynomials R and S so that we have the Eq. (23) called Bezout equation.

$$D(s) = A(s).S(s) + B(s).R(s) \quad (23)$$

Where B(s)/A(s) is the transfer function of the system.

$$\frac{B(s)}{A(s)} = \frac{MV_s}{L_s(R_r + sL_r\sigma)} \quad (24)$$

We can then develop a linear system of four equations resulting from the Bezout equation.

$$\begin{cases} A(s) = a_1 s + a_0 = sL_s L_r \sigma + L_s R_r \\ B(s) = b_0 = MV_s \\ R(s) = r_1 s + r_0 \\ S(s) = s_2 s^2 + s_1 s + s_0 \\ D(s) = d_3 s^3 + d_2 s^2 + d_1 s + d_0 \end{cases} \quad (25)$$

According to the pole placement technique, the polynomial D can be written as [22-23]:

$$D(s) = C.F = (s - s_c)(s - s_f)^2$$

$$D(s) = s^3 + (s_c + 2s_f)s^2 + ({s_f}^2 + 2s_c s_f)s + s_c {s_f}^2 \quad (26)$$

With $s_c$ is the pole of the control polynomial C and $s_f$ is the double pole of the filtering polynomial F.

Where:

The role of the control pole is to accelerate the system, it is chosen arbitrarily, greater than the pole of the polynomial A ($s_A$) [10], we chose:

$$s_c = 5\, s_A$$

Where:

$$s_A = -\frac{R_r}{L_r \sigma} \quad (27)$$

In order to enhance the robustness of the regulator, we choose $s_f$ three times greater than $s_c$:

$$s_f = 3\, s_c = 15\, s_A$$

We get the coefficients of polynomial D which are related to coefficients of polynomial R and S by the Sylvester matrix [22].

$$\begin{bmatrix} d_3 \\ d_2 \\ d_1 \\ d_0 \end{bmatrix} = \begin{bmatrix} a_1 & 0 & 0 & 0 \\ 0 & a_1 & 0 & 0 \\ 0 & a_0 & b_0 & 0 \\ 0 & 0 & 0 & b_0 \end{bmatrix} \begin{bmatrix} s_2 \\ s_1 \\ r_1 \\ r_0 \end{bmatrix} \quad (28)$$

According to equation (25), (26) and (28) we deduce the RST controller's parameters:

$$\begin{cases} d_3 = a_1 s_2 = 1 \\ d_2 = a_1 s_1 = s_c + 2s_f \\ d_1 = a_0 s_1 + b_0 r_1 = {s_f}^2 + 2s_c s_f \\ d_0 = b_0 r_0 = s_c {s_f}^2 \end{cases} \quad (29)$$

Therefore:

$$\begin{cases} s_2 = \frac{1}{L_s L_r \sigma} \\ s_1 = \frac{35 R_r}{L_s (L_r \sigma)^2} \\ s_0 = 0 \\ r_1 = \frac{340 {R_r}^2}{MV_s (L_r \sigma)^2} \\ r_0 = T = \frac{1125 {R_r}^3}{MV_s (L_r \sigma)^3} \end{cases} \quad (30)$$

Fig. 9 shows the RST control structure applied to the rotor side converter in order to control the stator active and reactive powers of the DFIG.

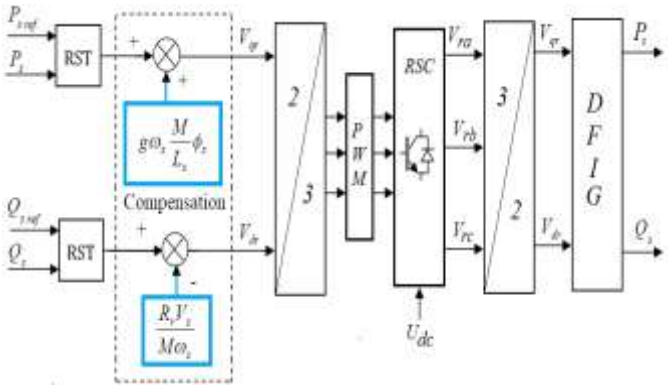


**Fig. 9.** Scheme of power control of DFIG using RST controller.

*3.3. ADRC Controller*

Consider a first order system time-varying dynamic system with single input denoted u, and single-output denoted y "Eq. (31)" [25-28].

$$\frac{dy}{dt} = f(y, d, t) + b_0 u \quad (31)$$

Where **f(y,d,t)** represents the combined effect of internal dynamics and external disturbance, $\mathbf{b_0}$ is parameter gain to estimate and **d** represents the external disturbance.

The following mathematical system "Eq. (32)" describes the state space of the process as [11, 25-28]:

$$\begin{cases} \dot{x}_1 = x_2 + b_0 u \\ x_2 = f \\ y = x_1 \end{cases} \quad (32)$$

The system of equations "Eq. 33" presents the state-space representation of the extended state observer (ESO) [11, 26].

$$\begin{cases} \dot{\hat{x}}_1 = \hat{x}_2 + \beta_1 (y - \hat{x}_1) + b_0 u \\ \dot{\hat{x}}_2 = \beta_2 (y - \hat{x}_1) \end{cases} \quad (33)$$

Where: [$\beta_1$, $\beta_2$] is the vector of the observer gain values [27].

$$\begin{bmatrix} \beta_1 \\ \beta_2 \end{bmatrix} = \begin{bmatrix} -2S_{ESO} \\ S_{ESO}^2 \end{bmatrix} \quad (34)$$

$\mathbf{S_{ESO}}$ is the pole of the observer is defined by the technique of placement of the poles.

The control input is given by the following equation [11, 26]:

$$u = \frac{u_0 - \hat{f}}{b_0} = \frac{u_0 - \hat{x}_2}{b_0} \quad (35)$$

Where, the plant can be controlled by a simple proportional controller "Eq. (36)" with gain values $\mathbf{K_P}$. The input signal reference denoted **r** [11, 26].

$$u_0 = K_p (r - \hat{y}) = K_p (r - \hat{x}_1) \quad (36)$$

Where, $K_p = S_{CL}$. Where, $S_{CL}$ denotes the desired closed loop pole.

Usually the controller regulation is done by observing the desired closed loop pole. Generally, $S_{ESO} = 3\sim7\ S_{CL}$ and consequently, $S_{CL}$ is the only setting parameter [11].

Figure 10 (a) and (b) show respectively the structure of the linear ADRC controller for a first order system and the structure of the ESO.

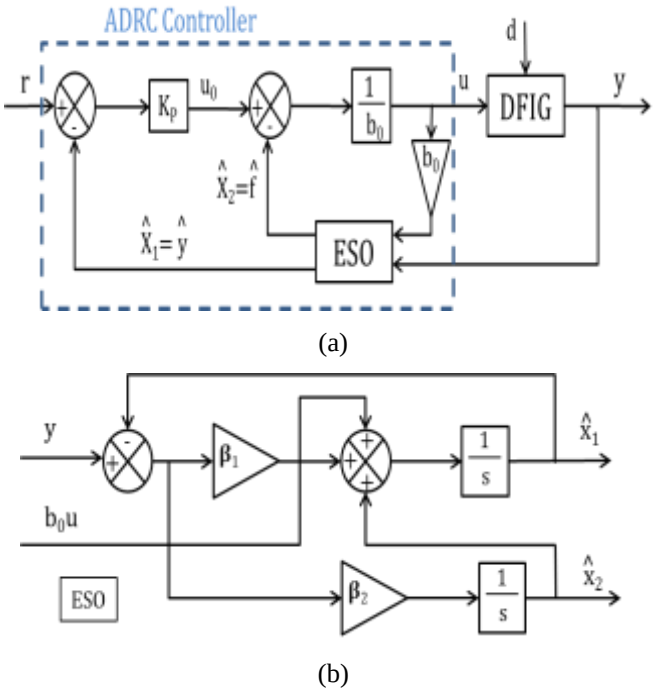


**Fig. 10.** (a) Structure of ADRC controller, (b) structure of the ESO.

The direct and quadratic rotor current is controlled by the controller ADRC, by imposing reference voltages direct and quadratic of the rotor to the RSC converter which generates the control signals using the Pulse Width Modulation (PWM) [11, 28].

The direct and quadratic current of the rotor currents are rearranged to be in the following form:

$$\begin{cases} \frac{dI_{rd}}{dt} = -\frac{R_r}{\sigma L_r} I_{rd} + \omega_r I_{rq} + \frac{1}{\sigma L_r} V_{rd} \\ \frac{dI_{rq}}{dt} = -\frac{R_r}{\sigma L_r} I_{rq} - \omega_r I_{rd} - \omega_r \frac{M}{\sigma L_r L_s} \phi_{sq} + \frac{1}{\sigma L_r} V_{rd} \end{cases} \quad (37)$$

We can write these expressions in the following form:

$$\frac{dI_{rd}}{dt} = f(I_{rd}, d, t) + b_0 u(t) \quad (38)$$

Where:

$$\begin{cases} f(I_{rd}, d, t) = -\frac{R_r}{\sigma L_r} I_{rd} + \omega_r I_{rq} + (\frac{1}{\sigma L_r} - b_0) V_{rd} \\ u(t) = V_{rd} \qquad \text{and} \qquad b_0 = \frac{1}{\sigma L_r} \end{cases} \quad (39)$$

In the same way:

$$\frac{dI_{rq}}{dt} = f(I_{rq}, d, t) + b_0 u(t) \quad (40)$$

Where:

$$\begin{cases} f(I_{rq}, d, t) = -\frac{R_r}{\sigma L_r} I_{rq} - \omega_r I_{rd} - \omega_r \frac{M}{\sigma L_r L_s} \phi_{sq} + (\frac{1}{\sigma L_r} - b_0) V_{rd} \\ u(t) = V_{rq} \qquad \text{and} \qquad b_0 = \frac{1}{\sigma L_r} \end{cases} \quad (41)$$

Figure 11 shows the ADRC control structure applied to the rotor side converter in order to control the stator active and reactive powers of the DFIG.

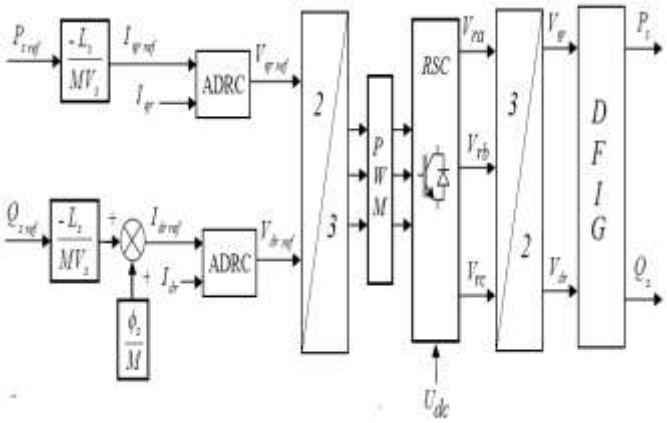


**Fig. 11.** Scheme of power control of DFIG using ADRC controller

## 4. Simulation with MATLAB/Simulink and Results

The simulation was carried out with MATLAB/Simulink, in order to validate the control strategies studied in this work and compare their performances.

The wind speed is modeled in the determinist form by a sum of several harmonics, according to [4], its expression is given by the following equation:

$$v(t) = v_0 + \sum_{k=1}^{i} a_k \sin(b_k \omega t) \quad (42)$$

Where $a_k$ and $b_k.\omega$ are respectively the amplitude and the pulsation of the harmonic of order k.

We chose:

$$v(t) = v_0 + 2\sin(\omega t) - 1.75\ \sin(3\omega t) + 1.5\sin(5\omega t) - 1.25\sin(10\omega t) + \sin(30\omega t) + 0.5\sin(50\omega t) + 0.25\sin(100\omega t) \quad (43)$$

Where $v_0$ is the average wind speed and $\omega=2\pi/10$

The Figure 12 shows the simulated wind profile with an average speed of 4.5 m/s, this figure shows that the turbine has a good adaptation to the variation of the wind thanks to the MPPT control.

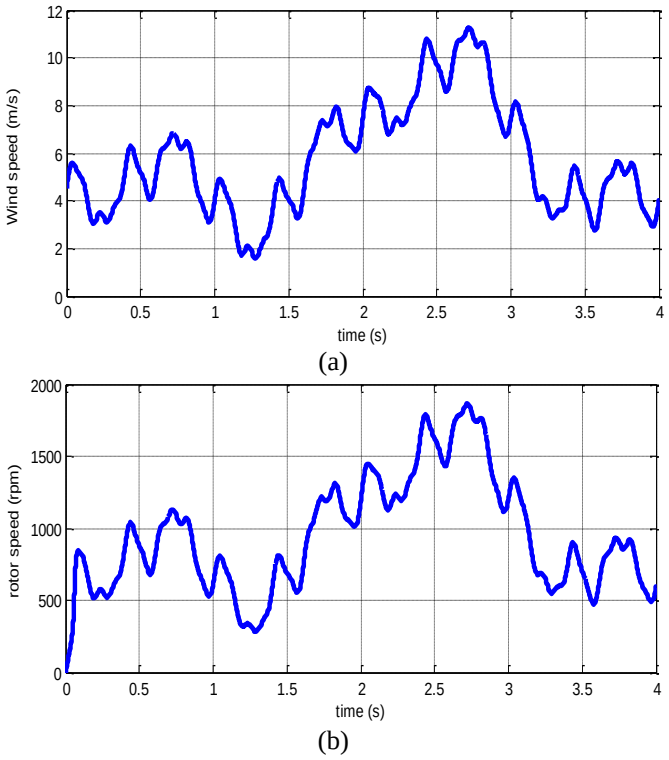


**Fig. 12.** Wind Speed and Mechanical Rotor Speed

The active stator power "Fig.13" has the same variation as that of the wind speed. we also note that the active power is negative which means that the MADA produces energy and supplies it to the grid.

The reference reactive power is chosen as follow "Fig. 14":

- From t=0 to t=0.5s : $\mathbf{Q_{s\text{-}ref}=0\ VAR}$
- From t=0.5 to t=1s: $\mathbf{Q_{s\text{-}ref}=-5e5VAR}$
- From t=1 to t=1.5s: $\mathbf{Q_{s\text{-}ref}=0VAR}$

### *4.1. Test of reference tracking*

The "Fig .13" and "Fig .14" illustrate respectively the active and reactive power variations of stator obtained by using the three control stratgies PI, RST and ADRC. The stator powers converges and tracks perfectly as their references ($P_{s\text{-}ref}$, $Q_{s\text{-}ref}$), but with a simple static error and with an important response time for the PI controller compared to the other controllers ($T_{PI}$=200 ms, $T_{ADRC}\approx T_{RST}$=30 ms). We can also note that the response of the active power is slow for the PI controller, this shows that the random and fast variation of the reference active power affect the performance of this controller. Therefore it can be concluded that the RST and ADRC controllers have a very good and high performance for this test "Table 1.".

**Table 1.** The system responses Parameters.

| Type of Controller | PI | RST | ADRC |
|---|---|---|---|
| Rise Time (s) | 0.030 | 0.028 | 0.028 |
| Settling time (s) | 0.2 | 0.03 | 0.03 |
| Overshoot (%) | 3.2 | 0 | 0 |
| Steady state error (%) | 1.25 | 0.06 | 0.06 |

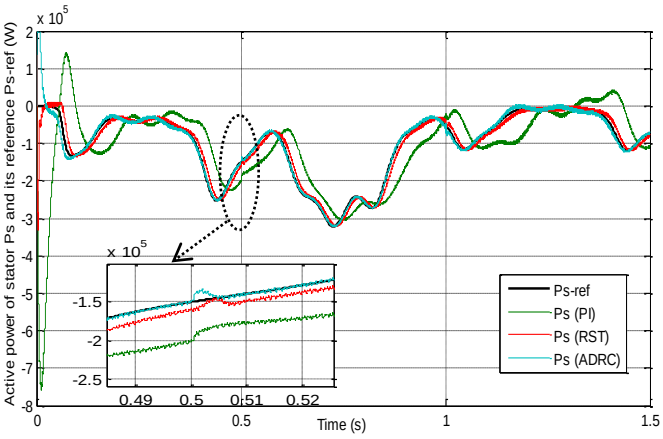


**Fig. 13.** Active power of stator and its reference.

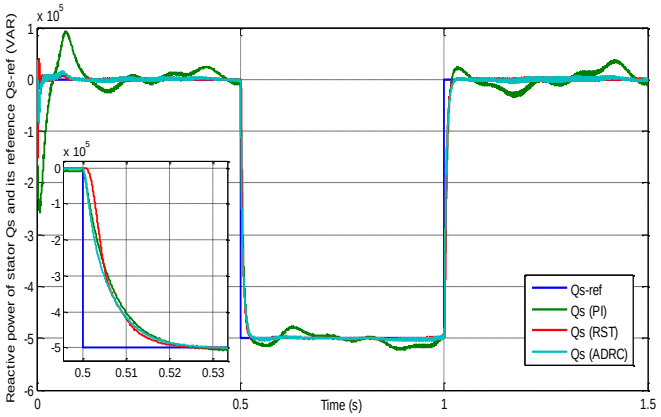


**Fig. 14.** Reactive power of stator and its reference.

### *4.2. Test of robustness*

This test is to examine the robustness of the three controllers by varying the internal DFIG parameters with increasing the resistance $R_r$ by 100%, Then the values of the rotor and stator inductance ($L_s$, $L_r$) are increased by 10% of their rated values.

The "Fig. 15" and "Fig. 16" show that the increase in the resistance of rotor $R_r$ of DFIG have not almost any influence for the three control stratgies, and the stability has not affected by these variation.

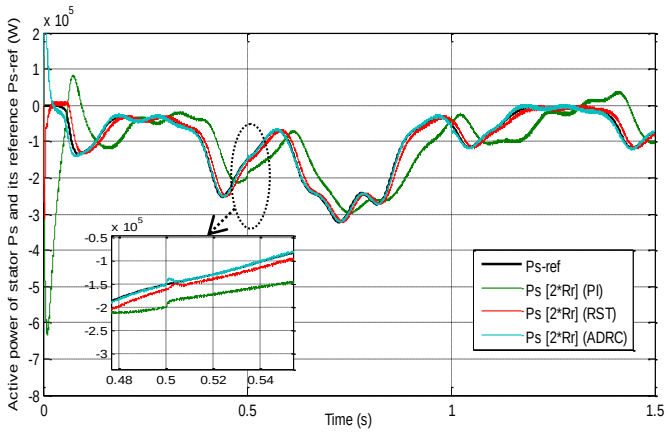


**Fig. 15.** Active power of stator for R'r=2Rr.

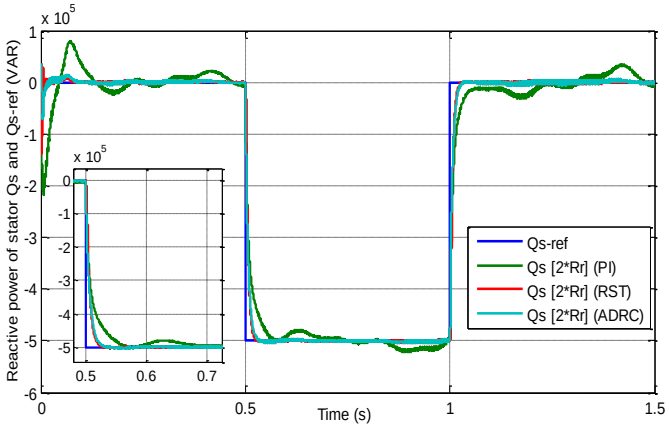


**Fig. 16.** Reactive power of stator for $R'_r=2R_r$.

By increasing the inductance value of the rotor Lr by 10% from its rated value. Figures 17 and figure 18 show the effect of this variation on the response of the active and reactive power of stator. It can be seen that the reactive power response with ADRC controller has a smaller overshoot of 10 % when compared to RST controller which has an overshoot of 18.3 % and to PI controller which has an overshoot of 24 %. In adition, with the ADRC controller, the oscillations are damped more quickly compared to the other controllers.

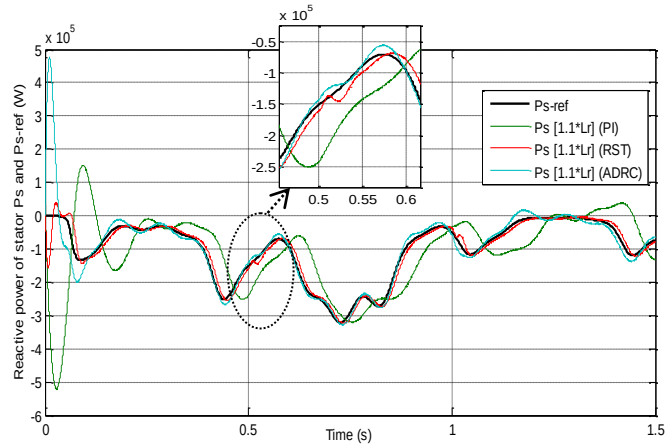


**Fig. 17.** Active power of stator for $L'_r=1.1L_r$.

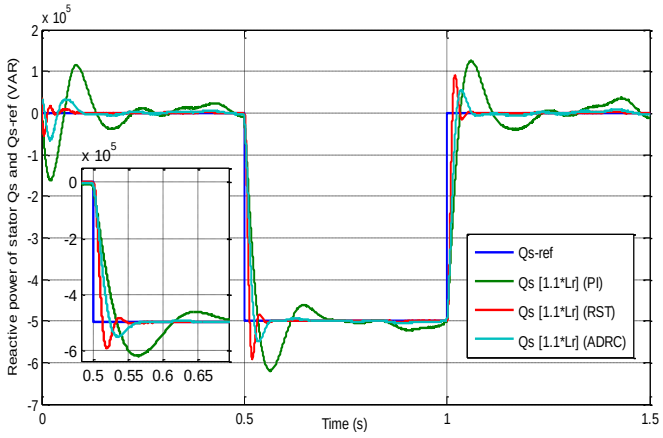


**Fig. 18.** Reactive power of stator for $L'_r=1.1L_r$.

Figure 19 and figure 20 show simulation results when the rotor and stator inductance (Ls, Lr) change at the same time (Ls+10%, Lr+10%) .these variation of two parameters deteriorates almost completely the performance of the PI controller. unlike the ADRC and RST controllers present an increase in response time ($T_{ADRC}\approx T_{RST}$=135 ms), but with little oscillations and smaller overshoot for the ADRC control strategy "Table 2.".

From simulation results of this test, we note that the ADRC controller is more robust, that has good robustness against parametric variations, compared to RST and PI controllers.

**Table 2.** The system responses Parameters.

| Type of Controller | PI | RST | ADRC |
|---|---|---|---|
| Rise Time (s) | 0.047 | 0.017 | 0.027 |
| Settling time (s) | 0.35 | 0.14 | 0.14 |
| Overshoot (%) | 32.9 | 32.1 | 21 |
| Steady state error (%) | 1.25 | 0.06 | 0.06 |

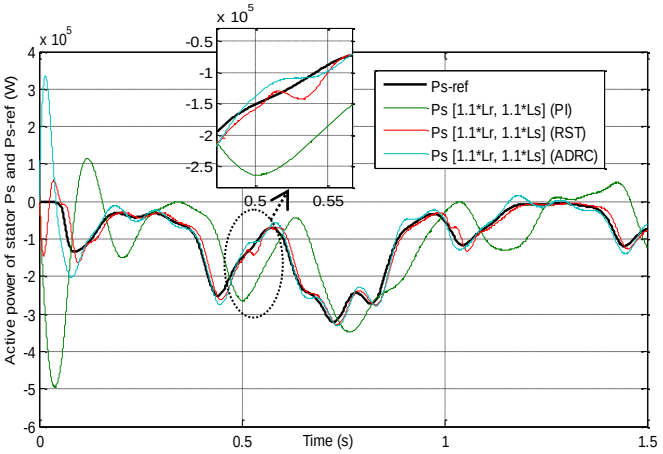


**Fig. 19.** Active power of stator for $L'_r=1.1L_r$ and $L'_s=1.1L_s$.

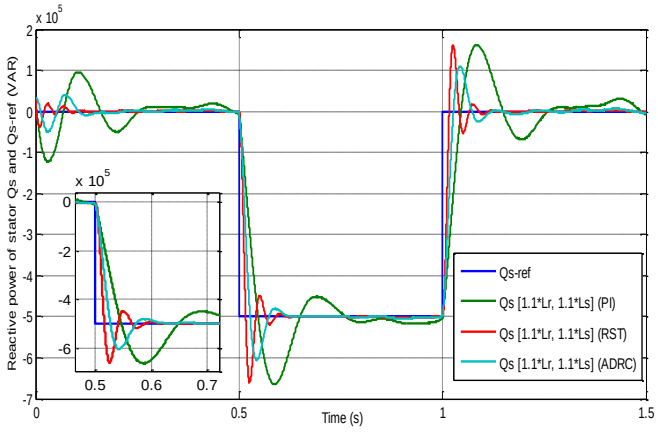


**Fig. 20.** Reactive power of stator for $L'_r$=1.1Lr and $L'_s$=1.1Ls.

## 5. Conclusion

In this work, we presented the modeling of a wind energy conversion system based on a doubly fed induction generator connected to grid. we developed and presented a comparative study of the three control strategies PI, RST and ADRC. These controllers are applied to the rotor side converter in order to control the active and reactive power exchanged between the stator of the generator and the grid. Where, the reference active power is provided by the MPPT (Maximum Power Point Tracking) block diagram.

Finally, the simulation result allows us to conclude that the active disturbance rejection (ADRC) and polynomial RST controllers are very efficient in term of tracking performances compared to conventional PI controller. But, in term of robustness, the ADRC controller is more robust to internal parameters changes compared to the two other controllers, because this control strategy delete in real time the effect of all disturbances which can affect our system.

## Appendix

**Table 3.** DFIG Parameters

| | |
|---|---|
| Rated power | 1.5 MW |
| Number of pole pairs p | 2 |
| Rated stator voltage | 398/690 V |
| Stator resistance $R_s$ | 0.012 Ω |
| Rotor resistance $R_r$ | 0.021 Ω |
| Stator inductance $L_s$ | 0.0137 H |
| Rotor inductance $L_r$ | 0.01367 H |
| Mutual inductance M | 0.0135 H |
| Nominal frequency f | 50 Hz |
| DC link voltage $U_{dc}$ | 1200V |

**Table 4.** Turbine Parameters

| | |
|---|---|
| Density of Air | 1.5 MW |
| Damping coefficient $f_v$ | 0.0024 |
| Moment of inertia J | 10 kg.m$^2$ |
| Optimal tip speed ratio $\lambda_{opt}$ | 8.2 |
| Maximal power coefficient $C_{Pmax}$ | 0.49 |
| Turbine diameter D | 70.5 m |
| Gain multiplier G | 90 |

**Table 5.** PI and ADRC Controllers Parameters

| | |
|---|---|
| **PI** controller | |
| Gain of proportional action $k_p$ | $1.0121\times10^{-4}$ |
| Gain of integral action $k_i$ | 0.0053 |
| **ADRC controller** | |
| Parameter gain $b_0 = 1/\sigma L_r$ | 2517 |
| Controller gain $K_p = S_{CL}$ | 120 |
| Pole of the ESO $S_{ESO} = 5S_{CL}$ | 600 |
| Extended state observer gains (ESO) | $\beta_1$=1200 |
| | $\beta_2$=360000 |

## References

[1] B. Beltran, T. Ahmed-Ali, M.E. Benbouzid, "Sliding Mode Power Control of Variable Speed Wind Energy Conversion Systems", IEEE Transactions on Energy Conversion, vol.23, pp. 551-558, 2008.

[2] S. El Aimani, "Modeling and Control structures for Variable Speed Wind Turbine", In: IEEE International Conference on Multimedia Computing and Systems (ICMCS), Ouarzazate, Morocco, pp. 1-5, 2011.

[3] M. Benbouzid, "High-Order Sliding Mode Control of DFIG-Based Wind Turbines", In: N. Luo, Y. Vidal, L. Acho (eds.) Wind Turbine Control and Monitoring. Springer, Cham, pp. 23-48, 2014.

[4] S. Mensou, A. Essadki, T. Nasser, B. Bououlid Idrissi, "An Efficient Nonlinear Backstepping Controller Approach of a Wind Power Generation System Based on a DFIG", International Journal of Renewable Energy Research, vol. 7, No. 4, pp. 1520-1528, 2017.

[5] K.S. Srikanth, G. Naga Sai Babu, V. Marritboyina, "Controlling of DFIG Based Wind Turbine", International Journal of Pure and Applied Mathematics, Vol. 114, 293-301, 2017.

[6] M. El Azzaoui, H. Mahmoudi, C. Ed-dahmani, and K. Boudaraia, "Comparing Performance of PI and Sliding Mode in Control of Grid Connected Doubly Fed Induction Generator", IEEE, International Renewable and Sustainable Energy Conference (IRSEC), Marrakech, Morocco, pp. 769 - 774, 2016.

[7] M. Nadour, A. Essadki, T. Nasser, "Comparative Analysis between PI & Backstepping Control Strategies of DFIG Driven by Wind Turbine", International Journal of Renewable Energy Research, vol. 7, No. 3, pp. 1307-1316, 2017.

[8] B. Hamane, M.L. Doumbia, A.M. Bouhamida, M. Benghanem , "Direct Active and Reactive Power Control of DFIG based WECS using PI and Sliding Mode Controllers", 40th Annual Conference of the IEEE Industrial Electronics Society (IECON), Dallas, TX, USA, pp. 2050-2055, 2014.

[9] F. Hachicha, L. Krichen, "Performance Analysis of a Wind Energy Conversion System Based On A Doubly-Fed Induction Generator", 8th IEEE International Multi-Conference on Systems, Signals & Devices, Sousse, Tunisia, pp. 1-6, 2011.

[10] B. Hamane, M. L. Doumbia, M. Bouhamida, A. Draou, H. Chaoui and M. Benghanem, "Comparative Study of PI, RST, Sliding Mode and Fuzzy Supervisory Controllers for DFIG based Wind Energy Conversion System", International Journal of Renewable Energy Research, vol. 5, No.4, pp. 1174-1185, 2015.

[11] M. Arbaoui, A. Essadki, T. Nasser, H. Chalawane, "Comparative Analysis of ADRC & PI Controllers Used in Wind Turbine System Driving a DFIG", International Journal of Renewable Energy Research, vol. 7, No. 4, pp. 1816-1824, 2017.

[12] Krishnat R. Dubal, Dattatray S. Chavan, "Maximum Power Point Tracking System for Wind Generator Using MATLAB", International Journal Of Engineering And Computer Science, Vol. 4 No. 1, pp. 10043-10050, 2015.

[13] J. Chen, L. Jiang, Wei Yao, Q. H. Wu, "A Feedback Linearization Control Strategy for Maximum Power Point Tracking of a PMSG Based Wind Turbine", IEEE International Conference on Renewable Energy Research and Applications (ICRERA), Madrid, Spain, pp. 79-84, 2013.

[14] L. P. Afonso, S. F. Pinto, J. F. Silva, "Maximum Power Point Tracker for Wind Energy Generation Systems using Matrix Converters", IEEE, 4th International Conference on Power Engineering, Energy and Electrical Drives (POWERENG13), Istanbul, Turkey, pp. 978-983, May 2013.

[15] E. Aydin, A. Polat, L. T. Ergene, "Vector Control of DFIG in Wind Power Applications", 5th IEEE International Conference on Renewable Energy Research and Applications (ICRERA), Birmingham, UK, pp. 478-483, 2016.

[16] O. Barambones, J. M. Gonzalez de Durana, E. Kremers, "Adaptive Robust Control to Maximizing the Power Generation of a Variable Speed Wind Turbine", IEEE International Conference on Renewable Energy Research and Applications (ICRERA), Madrid, Spain, pp. 167-172, 2013.

[17] A. L. L. F. Murari, J. A. T. Altuna, R. V. Jacomini, C. M. Rocha Osorio, J. S. S. Chaves and A. J. Sguarezi Filho, "A Proposal of Project of PI Controller Gains Used on the Control of Doubly-Fed Induction Generators", IEEE Latin America Transactions, vol. 15, No. 2, pp. 173-180, 2017.

[18] F. Senani, A. Rahab, F. Louar, F. Bourourou, H. Benalla, "Active and reactive power control of DFIG using PI and DPC controllers", IEEE, 4th International Conference on Electrical Engineering (ICEE), Boumerdes, Algeria, pp. 1- 6, 2015.

[19] L. Yang, G.Y. Yang, Z. Xu, Z.Y. Dong, K.P. Wong, and X. Ma, "Optimal Controller Design Of A Doubly-Fed Induction Generator Wind Turbine System For Small Signal Stability Enhancement", IET Generation, Transmission & Distribution, vol. 4(5), pp. 579–597, 2010.

[20] A. Tamaarat, A. Benakcha, "Performance of PI Controller for Control of Active and Reactive Power in DFIG Operating in a Grid connected Variable Speed Wind Energy Conversion System", Springer. Front. Energy, vol. 8, pp. 371–378, 2014.

[21] M. K. Bourdoulis, A. T. Alexandridis, "Rotor-side PI Controller Design of DFIG Wind Turbines based on Direct Power Flow Modeling", IEEE International Conference on Renewable Energy Research and Applications (ICRERA), Madrid, Spain, pp. 155-160, 2013.

[22] M. Laakam, L. Sbita, "RST Control of a Doubly-fed Induction Generator for Wind Energy Conversion", International Journal of Engineering Research & Technology (IJERT), vol. 3, No. 3, pp. 2507-2512, 2014.

[23] A. Elmansouri; J. El mhamdi; A. Boualouch, "Wind energy conversion system using DFIG controlled by back-stepping and RST controller", IEEE, International Conference on Electrical and Information Technologies (ICEIT), Tangiers, Morocco, pp. 312-318, 2016.

[24] E. El Hawatt, M. S. Hamad, K. H. Ahmed, I. F. El Arabawy, "Low voltage ride-through capability enhancement of a DFIG wind turbine using a dynamic voltage restorer with Adaptive Fuzzy PI controller", IEEE International Conference on Renewable Energy Research and Applications (ICRERA), Madrid, Spain, pp. 1234-1239, 2013.

[25] J. Han, "From PID to Active Disturbance Rejection Control", IEEE trans. on Industrial Electronics, vol. 56, pp. 900-906. IEEE Journals & Magazines, 2009.

[26] S. Wang, W. Tan, D. Li, "Design of Linear ADRC for Load Frequency Control of Power Systems with Wind Turbine", 14th IEEE International Conference on Control, Automation, Robotics and Vision (ICARCV), Dallas, TX, USA, pp. 1-5, 2016.

[27] G. Herbst, "A Simulative Study on Active Disturbance Rejection Control (ADRC) as a Control Tool for Practitioners", Electronics, vol. 2, pp. 246-279, 2013.

[28] A. Boukhriss, T. Nasser, A. Essadki, "A Linear Active Disturbance Rejection Control Applied For Dfig Based Wind Energy Conversion System", International Journal of Computer Science Issues (IJCSI), vol. 10, No. 2, pp. 391-399, 2013.